

# Journal Pre-proof

High-resolution anthropogenic ammonia emission inventory for the Yangtze River Delta, China

Xingna Yu, Li Shen, Xinhong Hou, Liang Yuan, Yuepeng Pan, Junlin An, Shuqi Yan



PII: S0045-6535(20)30535-X

DOI: <https://doi.org/10.1016/j.chemosphere.2020.126342>

Reference: CHEM 126342

To appear in: *ECSN*

Received Date: 15 June 2019

Revised Date: 17 February 2020

Accepted Date: 24 February 2020

Please cite this article as: Yu, X., Shen, L., Hou, X., Yuan, L., Pan, Y., An, J., Yan, S., High-resolution anthropogenic ammonia emission inventory for the Yangtze River Delta, China, *Chemosphere* (2020), doi: <https://doi.org/10.1016/j.chemosphere.2020.126342>.

This is a PDF file of an article that has undergone enhancements after acceptance, such as the addition of a cover page and metadata, and formatting for readability, but it is not yet the definitive version of record. This version will undergo additional copyediting, typesetting and review before it is published in its final form, but we are providing this version to give early visibility of the article. Please note that, during the production process, errors may be discovered which could affect the content, and all legal disclaimers that apply to the journal pertain.

© 2020 Published by Elsevier Ltd.

## CRediT author statement

Xingna Yu: Conceptualization, Writing- Reviewing and Editing, Supervision

Li Shen: Methodology, Software

Xinhong Hou: Investigation

Liang Yuan: Formal analysis

Yuepeng Pan: Resources

Junlin An: Resources

Shuqi Yan: Formal analysis

Journal Pre-proof

1 High-resolution anthropogenic ammonia emission inventory for the Yangtze River

2 Delta, China

3 Xingna Yu<sup>1,\*</sup>, Li Shen<sup>1,2</sup>, Xinhong Hou<sup>1</sup>, Liang Yuan<sup>3</sup>, Yuepeng Pan<sup>4</sup>, Junlin An<sup>1</sup>, Shuqi Yan<sup>1</sup>

4 <sup>1</sup> Key Laboratory of Meteorological Disaster, Ministry of Education (KLME)/Joint International

5 Research Laboratory of Climate and Environment Change (ILCEC)/Collaborative Innovation

6 Center on Forecast and Evaluation of Meteorological Disasters (CIC-FEMD)/Key Laboratory for

7 Aerosol-Cloud-Precipitation of China Meteorological Administration, Nanjing University of

8 Information Science and Technology, Nanjing 210044, China

9 <sup>2</sup> China Eastern Airlines Corporation Limited, Operations & Customer Center,

10 Shanghai 201100, China

11 <sup>3</sup> College of Atmospheric Science, Chengdu University of Information Technology, Chengdu

12 610225, China

13 <sup>4</sup>State Key Laboratory of Atmospheric Boundary Layer Physics and Atmospheric Chemistry

14 (LAPC), Institute of Atmospheric Physics (IAP), Chinese Academy of Sciences (CAS), Beijing

15 100029, China

16

17

18 \*Corresponding author

19 E-mail address: xnyu@nuist.edu.cn

20

21

22

23 **Abstract:** The Yangtze River Delta (YRD) is one of the regions with air pollution and high  
24 ammonia ( $\text{NH}_3$ ) emission in China. A high-resolution ammonia emission inventory for the YRD  
25 region was developed based on the updated source-specific emission factor (EFs) and the  
26 county-level activity data. The  $1 \times 1$  km gridded emissions were allocated by using the appropriate  
27 spatial surrogate. The total  $\text{NH}_3$  emissions changed insignificantly from 2006 to 2014 and varied  
28 in the range of 981.65 kt - 1014.30 kt. The fertilizer application and livestock were the major  
29 contributors of total emission. Humans, biomass burning and vehicles were the top three  
30 contributors of non-agricultural sources, accounting for 37.24%, 31.02% and 10.85%, respectively.  
31 Vehicles were calculated to be the non-agricultural source with the fastest annual growth rate.  $\text{NH}_3$   
32 emissions from the nitrogen fertilizer application generally peaked in summer, corresponding to  
33 the planting schedule and relatively high temperature. High  $\text{NH}_3$  emissions occurred in the north  
34 as opposed to low emissions in the south of the YRD. The cities of Xuzhou, Yancheng and  
35 Nantong with more agricultural activities were demonstrated to have relatively high  $\text{NH}_3$   
36 emissions, contributing 10.0%, 9.0 and 7.1% of total emissions, respectively. The validity of the  
37 emission estimates was further evaluated based on the uncertainty analysis by Monte Carlo  
38 simulation, comparison with previous studies, and correlation analysis between  $\text{NH}_3$  emission  
39 density and observed ground  $\text{NH}_3$  concentration. A detailed  $\text{NH}_3$  emission inventory is the basis of  
40 regional-scale air quality model simulation and can provide valuable information for  
41 understanding the formation mechanism of pollutants.

42

43 **Keywords:** Ammonia ( $\text{NH}_3$ ); Emission inventory; Spatial distribution; Evaluation

44

## 45 1. Introduction

46 Ammonia ( $\text{NH}_3$ ) is one of the most important trace gases in the atmosphere and has an  
47 important impact on the atmospheric environment and ecosystem. As the most abundant alkaline  
48 gas in the atmosphere,  $\text{NH}_3$  can easily react with  $\text{NO}_x$  and  $\text{SO}_2$  in the atmosphere and produce  
49 ammonium forms, such as  $(\text{NH}_4)_2\text{SO}_4$ ,  $\text{NH}_4\text{HSO}_4$ ,  $\text{NH}_4\text{NO}_3$  and  $\text{NH}_4\text{Cl}$ . These forms of  
50 ammonium are important components of fine aerosol particles (Wang et al., 2011; Wu et al., 2015),  
51 which can cause aerosol pollution and can affect atmospheric visibility.  $\text{NH}_3$  can also accelerate  
52 the nucleation process of sulphate particles, thus contributing to the formation of cloud  
53 condensation nuclei. In addition, most gaseous ammonia and particulate ammonium can be  
54 returned to soil or water by wet and dry deposition, which may lead to the acidification of soil,  
55 eutrophication of water and even a decrease in biological diversity (Anderson et al., 2003; Krupa,  
56 2003; Matson et al., 2002). Although China has attached great importance to the treatment of air  
57 pollution,  $\text{NH}_3$  was not a monitoring project stipulated in the National Environmental Air Quality  
58 Standard (<http://www.mee.gov.cn/>). There are various pollution sources of  $\text{NH}_3$  due to the lack of  
59 corresponding reduction targets, causing sources such as industry and agriculture to discharge  $\text{NH}_3$   
60 without restraint.

61 The previous study indicated that the ammonium contributed approximately 23% and 17% of  
62 the total ion concentration in Nanjing and Shanghai, while this ratio reached 29% during the haze  
63 event in Suzhou, which significantly drove the formation of  $\text{PM}_{2.5}$  during air pollution episodes in  
64 the YRD (Chen, 2017; Tian et al., 2016; Yu et al., 2019). For deposition of nitrogenous species,  
65 the study showed that nitrogen deposition was dominated by deposition of reduced nitrogen  
66 ( $\text{NH}_3+\text{NH}_4^+$ ), which contributed approximately 67% to the total flux (Pan et al., 2012). The  $\text{NH}_3$

67 dry deposition flux in Nanjing was  $855.03 \mu\text{g m}^{-2} \text{h}^{-1}$  in 2017 and  $1273.20 \mu\text{g m}^{-2} \text{h}^{-1}$  in 2018,  
68 respectively (Zhao, 2019). Because  $\text{NH}_3$  plays a key role in the formation of fine particle and  
69 nitrogen deposition, a detailed and accurate inventory of  $\text{NH}_3$  are crucial to the control strategies  
70 of particulate pollution, and the guidance of  $\text{NH}_3$  limitation measures.

71 Since the early 1990s, many scholars have performed considerable research on ammonia  
72 emission inventories from anthropogenic sources (Battye et al., 2003; Olivier et al., 1998) and  
73 natural sources (Sarwar et al., 2005; Van et al., 1998). According to the EEA's (European  
74 Economic Area)  $\text{NH}_3$  assessment report in 2013, the total  $\text{NH}_3$  emissions of EEA member  
75 countries were calculated to be 428 wt in 2011, and agricultural sources accounted for 93.7% of  
76 the total emission. The  $\text{NH}_3$  emission inventories indicated that nitrogen fertilizer application and  
77 livestock contributed more than 57% of global emissions (Bouwman et al., 1997) and more than  
78 80% of the total  $\text{NH}_3$  emissions in China (Kang et al., 2016; Zhou et al., 2015). Compared to  
79 agricultural sources, ammonia emissions from non-agricultural sources (including human  
80 excrement, traffic, waste treatment, industries and fossil burning) were calculated to be 739.6 kt,  
81 accounting for approximately 7.5% of the total ammonia emissions (Huang et al., 2012).  $\text{NH}_3$   
82 emission inventories have been established on various levels, such as national scale (Kang et al.,  
83 2016; Huang et al., 2012; Zhang et al., 2018), and regional scale, including the North China Plain  
84 (Zhang et al., 2010), the Beijing-Tianjin-Hebei (Zhou et al., 2015), the Pearl River Delta (Zheng et  
85 al., 2012), and the YRD (Dong et al., 2009), and also some provincial scale including Henan,  
86 Fujian and Sichan (Feng et al., 2015; Wang et al., 2018; Wu et al., 2017). However, previous  
87 emission inventories do not entirely reflect the local emission characteristics. The reason can be  
88 attributed to low-resolution activity data, the incomplete  $\text{NH}_3$  emission sources and different

89 emission factors.

90 With the rapid development of industrialization and urban agglomeration, the regional  
 91 secondary pollution is becoming more serious in the YRD region. The prior study of ammonia  
 92 emission cannot meet the needs of the current study on regional air quality and acid deposition.  
 93 Therefore, a comprehensive NH<sub>3</sub> emission inventory in the YRD (25 cities) with high resolution  
 94 and a 1 km × 1 km gridded emission allocation were developed in 2014 based on the activity data  
 95 and emission factors of various ammonia emission sources.

## 96 2. Method and data

97 In this study, fertilizer application and livestock were regarded as agricultural sources. The  
 98 non-agricultural sources included humans, the chemical industry, fossil burning, biomass burning,  
 99 garbage treatment, sewage treatment, vehicles, pets and urban grassland.

100 NH<sub>3</sub> emissions of each source were calculated as a product of the activity data and specific EFs,  
 101 according to the following equation (1):

$$102 \quad E = \sum_i \sum_j (A_{i,j} \times EF_{i,j}) \quad (1)$$

103 where  $E$  is total NH<sub>3</sub> emissions,  $i, j$  represent the source type and prefecture-level city  
 104 respectively,  $A_{i,j}$  is the activity data, and  $EF_{i,j}$  is the corresponding  $EF$ . The activity data of  
 105 each source are derived from the local statistical yearbooks. The emissions factors are mainly  
 106 adopted from the Technical Guidelines for Preparation of Atmospheric Ammonia Emissions  
 107 Inventory from Ministry of Ecology and Environment of the People's Republic of China (2014) as  
 108 well as domestic and foreign research results, and the former is preferred.

### 109 2.1 Agricultural source

#### 110 2.1.1 Synthetic fertilizer application

111 Nitrogen fertilizer contains elemental nitrogen that is applied to crops.  $\text{NH}_3$  is discharged into  
 112 the atmosphere through microbial action or decomposition, resulting in significant volatilization of  
 113  $\text{NH}_3$  in farmland areas. In general,  $\text{NH}_3$  emissions from fertilizer are a function of the fertilizer  
 114 type, soil properties (pH values, water content, calcium content, etc.), meteorological conditions  
 115 (temperature, precipitation, and wind speed), application rate and method of application (injection  
 116 or surface). In this study, we classified the synthetic fertilizers used in the YRD region as urea,  
 117 ammonium bicarbonate (ABC), ammonium nitrate (AN), ammonium sulphate (AS), and other  
 118 fertilizers (compound fertilizer related to  $\text{NH}_3$  emissions were also considered, such as  
 119 three-nutrient compound fertilizer and ammonium phosphate). In the statistical yearbooks, the first  
 120 four types are classified as N fertilizer, while the other fertilizers are classified as phosphate  
 121 fertilizer and compound fertilizer, respectively. The ratios of different fertilizer applications are  
 122 listed in Table S1.

123 According to the method used in the National Ammonia Strategy Evaluation System  
 124 (NARSES) N fertilizer module (DEFRA, 2001), the emission factor for fertilizer type is modified  
 125 by functions relating to soil pH, land use, application rate, rainfall and temperature. The  $EF$  for a  
 126 given scenario is calculated according to formula (2):

$$127 \quad EF = EF_{MAX} \times RF_{PH} \times RF_T \times RF_{rain} \times RF_{rate} \times RF_{landuse} \quad (2)$$

128 where  $EF_{max}$  is the highest emission associated with each fertilizer type,  $RFs$  represents the  
 129 reduction factors expressed as a proportion.

130 The  $EF_{max}$  for urea AS and ABC were considered to be 45%, while 4% for AN and other  
 131 nitrogen fertilizers (Zhang and Luan, 2009). When ammonium nitrate was applied to lime soil and  
 132 other soils, the  $RF_{PH}$  was considered to be 1 and 0.0889, respectively (Wang et al., 2018). The



133  $RF_{pH}$  was also considered to be 1 when other types of nitrogen fertilizer were applied to all  
 134 soils.

135 Because the partial pressure of  $NH_3$  in solution increases exponentially with temperature,  
 136 temperature is likely to be the most important meteorological factor for synthetic fertilizer  
 137 application. According to the characteristics of temperature distribution in China, the  $RF_T$  of the  
 138 original NARSES model was not suitable for the YRD region. Therefore, we used the modified  
 139 functions for the estimation of ammonia volatilization associated with nitrogen fertilizer (Zhang et  
 140 al., 2011), and calculated the  $RF_T$  for non-calcareous soil and calcareous soil using equations (3)  
 141 and (4), respectively.

$$142 \quad RF_T = EXP(0.2197225 \times (T_{month} - T_{annual}) / 3) / 2 \quad (3)$$

$$143 \quad RF_T = EXP(0.1386 \times (T_{month} - T_{year}) / 3) / 2 \quad (4)$$

144 where  $T_{month}$  and  $T_{annual}$  are the local mean values of monthly and annual temperature, respectively,  
 145 and  $T_{year}$  is the mean annual temperature in China. The meteorological parameters were derived  
 146 from MICAPS (Meteorological Information Combine Analysis and Process System) ground  
 147 observation data.

148 When urea is applied to soil, it hydrolyses to produce ammonium bicarbonate, an unstable  
 149 compound that can quickly decompose to release gaseous  $NH_3$ . In the NARSES model, the  
 150 influence of land use on  $NH_3$  emissions was considered due to the reducing wind speed and  
 151 temperature at the soil surface. In this study, a value of 0.7 was used for  $RF_{landuse}$  for fertilizer  
 152 applications in maize fields (Zhang and Luan, 2009). The higher fertilizer application rate and the  
 153 pH value of soil surface causes a greater loss of  $NH_3$ .

154 2.1.2 Livestock and poultry

155 In this study, the ammonia emissions of livestock and poultry were estimated for each livestock  
156 category using headcount information at the county level and specific ammonia EFs. Livestock  
157 and poultry covered 9 subcategories: duck, chicken, rabbit, sheep, pig, buffalo, cattle, cow and  
158 beef cattle. The activity data of each subcategory was obtained from the China Rural Statistical  
159 Yearbook and local Statistical Yearbook, and detailed EFs for each animal listed in Table S7. We  
160 chose the number of stocks stored at the end of the year when the breeding period was longer than  
161 one year, while the number of slaughters was chosen for the livestock with a breeding period of  
162 less than one year.

## 163 2.2 Non-agricultural sources

164  $\text{NH}_3$  emissions from humans increase with the increase of the population. Generally,  $\text{NH}_3$   
165 emissions from humans include normal metabolic processes (respiration, perspiration and  
166 excretion). Population and sanitation are the key determinants of human  $\text{NH}_3$  emissions. In this  
167 study, due to the different sanitary conditions of the toilet systems in rural and urban areas,  $\text{NH}_3$   
168 emissions in rural and urban areas were considered separately.  $\text{NH}_3$  emissions from human were  
169 estimated by multiplying the year-end resident population in rural and urban areas by the  
170 corresponding emission factors (Shen, 2014).

171 Chemical industry sources include synthetic ammonia and nitrogen fertilizer production.  
172 Ammonia emissions were estimated using the city-level production output of industrial process,  
173 which was obtained from the local Statistical Yearbook and the corresponding EFs. The sources of  
174 ammonia in the combustion of fossil fuels mainly include natural gas, coal, gasoline, diesel, and  
175 kerosene.  $\text{NH}_3$  emissions from fuel combustion were calculated as the product of industrial and  
176 domestic consumption and specific EFs. Biomass burning sources include waste straw burning,

177 household straw burning, household firewood burning, and forest and grassland burning.  
 178 Considering the topography and vegetation of the YRD region, the NH<sub>3</sub> emissions from forest and  
 179 grassland fires were not considered. Based on the local cropping structure, a total of 7 crop types  
 180 were considered and divided into domestic burning and in-field burning in this study. The related  
 181 parameters of crop straw incineration were mainly selected from results related to the whole  
 182 country and the adjacent areas of the YRD region. The annual yield data of the main crops in each  
 183 city were obtained from the local Statistical Yearbook, and the total amount of pollutants  
 184 discharged from the open-air combustion of waste was calculated according to equation (5):

$$185 \quad E_i = \sum (P_{i,j} \times N_j \times F \times EF_j \times B_i) \quad (5)$$

186 where E is the ammonia emission, kt/a; i and j represent the area and crop type, respectively; P is  
 187 the annual yield of crops, t/a; N is the ratio of the crop straw amount to crop yield; B is the drying  
 188 ratio of straw; F is the burning rate of straw burning in open air; and EF is the ammonia emission  
 189 factor of crops. Because the recommended EFs for these crop residues are significantly different,  
 190 specific EFs are selected for each type of crop. The values of N, B, D and F are shown in Table  
 191 S2.

192 NH<sub>3</sub> emissions from sewage treatment mainly come from three processes: microbial absorption  
 193 in activated sludge of sewage treatment plants, nutrient treatment of digested sewage and sludge  
 194 spreading. Referring to Gu et al. (2012), we calculated the NH<sub>3</sub> emissions based on the sewage  
 195 discharge. Chinese Urban Construction Statistical Yearbook shows that waste disposal in the YRD  
 196 region includes incineration and landfill. We estimated the NH<sub>3</sub> emissions according to the amount  
 197 of domestic garbage disposal in each city. The NH<sub>3</sub> emissions from the waste incineration process  
 198 were calculated based on equation (1). Sutton et al. (2000) showed that NH<sub>3</sub> emissions produced

199 by landfills was considered to be 0.0073 times of methane emissions. The methane emissions can  
200 be calculated according to equation (6):

$$201 \quad E = MSW \times MCF \times DOC \times DOC_F \times F \times 16/12 \quad (6)$$

202 where E represents the methane emissions, t/a; MSW is the landfill amount of domestic garbage,  
203 t/a; MCF is a methane correction factor, i.e., 1.0; DOC and  $DOC_F$  represent the content of  
204 degradable organic carbon in waste and the decomposition percentage of degradable organic  
205 carbon; the recommended values from the IPCC are 9% and 77%, respectively;  $F$  is the content of  
206 methane in landfill gas with a value of 0.5; and  $16/12$  is the coefficient of carbon conversion to  
207 methane.

208 The exhaust emission of vehicle is an important  $NH_3$  source in urban areas. Considering the  
209 rapid increase in the vehicle population from 2006-2014 in the YRD, the  $NH_3$  emissions caused by  
210 on-road vehicles may change more significantly than that other non-agricultural sources. Activity  
211 data of vehicles are obtained by the Statistical Yearbook of Jiangsu, Shanghai and Zhejiang  
212 provinces. Referring to the classification by Zhang et al. (2013), a total of 9 vehicle types are  
213 considered in this study, and the definition of each vehicle type has been listed in Table S3.  
214 According to the technical guideline (Ministry of Ecology and Environment of the People's  
215 Republic of China, 2014), light-duty passenger vehicles, mini-duty passenger vehicles, light-duty  
216 truck and mini-duty truck are grouped into light-duty vehicles, and medium-duty passenger  
217 vehicles, heavy-duty passenger vehicles, medium-duty truck and heavy-duty truck are grouped  
218 into heavy-duty vehicles. According to vehicle classification and fuel type, motor vehicles can be  
219 divided into light gasoline vehicle, light gasoline truck, heavy gasoline vehicle, heavy gasoline  
220 truck, light diesel vehicle, light diesel truck, heavy diesel vehicle, heavy diesel truck and

221 motorcycle. Because the fuel type data for vehicle classification in past years are rather limited,  
222 we referred to the fuel type share of various vehicle fleets observed by Che (2010). The  $\text{NH}_3$   
223 emissions of on-road vehicles were the product of the number of vehicles, the total annual mileage  
224 and the specific EFs. The annual average mileage of vehicles and specific EFs were adopted by  
225 Che (2010) and Ministry of Ecology and Environment of the People's Republic of China (2014)  
226 (See Table S4). In this study, we did not consider the impact of vehicle driving cycle on specific  
227 EFs due to the lack of fleet average speed.

228  $\text{NH}_3$  emissions from pets and urban grasslands were also calculated according to the method  
229 reported by Wu et al. (2017). According to the report by Wu et al. (2015), an average of one in 13  
230 people keeps a pet in China, accounting for approximately 62% for dogs and 19% for cats,  
231 respectively. Homeless pets were not considered in this research. For urban grasslands, the annual  
232  $\text{NH}_3$  EF was 2.5% of the applied N fertilizer, and the EF was calculated to be  $5 \text{ kg ha}^{-1} \text{ yr}^{-1}$   
233 (Chinkin and Ryan, 2002). In this study, the emission data and factors of each source were  
234 summarized in Table S5, Table S6 and Table S7.

### 235 2.3 Spatial distribution of $\text{NH}_3$ emission

236 The  $1 \text{ km} \times 1 \text{ km}$  gridded  $\text{NH}_3$  emissions were established by the various sources based on  
237 ArcGIS software version 10.2 and different distribution modes (Wang et al., 2017a; Wang et al.,  
238 2017b). Based on the results of emission inventory, the gridded ammonia emission can be  
239 obtained by appropriate allocation factors. The spatial distribution area of anthropogenic ammonia  
240 was selected between the latitude of  $27.14^\circ\text{N}$  and  $35.12^\circ\text{N}$ , and between the longitude of  $116.35^\circ\text{E}$   
241 and  $122.95^\circ\text{E}$ . The  $1 \text{ km} \times 1 \text{ km}$  spatial resolution was set, covering Shanghai, Jiangsu Province  
242 and Zhejiang Province. Model domain information and central point coordinates are listed in S8

243 for the mapping of the several different emission sources and for estimating the total emissions.

244 The form of spatial distribution includes point, line and area sources distribution based on the

245 emission characteristics, spatial distribution and geographic information of emission sources. The

246 point sources are regarded as stationary emission sources such as nitrogen fertilizer production,

247 power plants and industrial boilers, while vehicle emission as the line source. The area sources

248 include nitrogen fertilizer application, livestock, fuel and biomass combustion, and urban green

249 land. The spatial allocation of point sources is to locate the emission to the corresponding grid

250 according to the longitude and latitude coordinates of each enterprise. The spatial distribution of

251 line source is based on the information of traffic road

252 (including the national road, provincial road, county road, and urban expressways). Firstly, all

253 kinds of road information are combined to calculate the total length of roads within the

254 administrative area of each city. Then, the total length of roads in grid cell is calculated according

255 to the defined grid. The ratio of the length of roads within the grid to the administrative area is

256 taken as the distribution factor, and the ammonia emission of traffic sources in 2014 is taken as the

257 distribution target to calculate the gridded ammonia emission. The allocation method from area

258 sources is similar to that of line sources. For livestock, emissions from free-range and intensive

259 livestock production were redistributed based on rural population density. Emissions from

260 fertilization application and urban greenland were allocated by type of land use. Emissions from

261 fuel combustion, pets, sewage treatment, garbage treatment and human waste were also regridded

262 on the basis of population distribution. The data of land use types, population grids and rural

263 residential area/land used in spatial distribution are from the National Earth System Science Data

264 Centre (<http://www.geodata.cn/index.html>).

## 265 2.3 Uncertainty analysis

266 Quantitative analysis has great importance for emission inventories and can help to identify  
267 sources with high uncertainty to help make pointed references for the inventory in future work  
268 (Streets et al., 2003). The uncertainty parameters and sources of probability distribution are as  
269 follows: 5% uncertainty for statistical data from the yearbook, 10% uncertainty for department  
270 survey data and 15% uncertainty for data estimated by experts. The input data can generally be  
271 considered to be a normal distribution when the uncertainty range is less than 60%. Therefore, we  
272 assumed that the activity data and emission factors followed a normal distribution. The  $\text{NH}_3$   
273 emission range was estimated using a Monte Carlo simulation, and we ran 10000 Monte Carlo  
274 simulations to estimate the  $\text{NH}_3$  emissions for each source. In this article, the lower limit range  
275 and upper limit range of the 95% confidence interval and the emission amount of each source  
276 were selected to calculate the uncertainty range.

277 2.4 Observed  $\text{NH}_3$  concentration and analysis

278 Ammonia can easily be converted into ammonium ( $\text{NH}_4^+$ ) by chemical reactions with acidic gas  
279 in the atmosphere. The concentration of ammonium observed in the environment can be used as  
280 the main chemical index for ammonia emission inventory assessment. Assuming that the emission  
281 of  $\text{NH}_3$  is separated simply and rapidly between gaseous  $\text{NH}_3$  and particulate  $\text{NH}_4^+$  or between  
282 gaseous  $\text{NH}_3$  and wet  $\text{NH}_4^+$ , the concentration of environmental  $\text{NH}_3$  on the ground can be directly  
283 related to the emission density of  $\text{NH}_3$  (Wang et al., 2018). Ambient  $\text{NH}_3$  was observed in Nanjing  
284 from September 2015 to August 2016 using ANALYST passive samplers. The samplers were  
285 installed on the rooftop of the Meteorology Building of Nanjing University of Information Science  
286 and Technology (NUIST, lat:  $32.2^\circ\text{N}$ , long:  $118.7^\circ\text{E}$ , 30 m). The ANALYST sampler for  $\text{NH}_3$  uses

287 a treated glass microfibre filter as an absorbent. Each sampler was exposed for one month.  
288 Samples were retained in their airtight vials and remained frozen in the laboratory refrigerator  
289 until they were analysed within one month. The samples were extracted and analysed according to  
290 the analysis method recommended by the manufacturer.  $\text{NH}_3$  was absorbed as ammonium by the  
291 samplers and was determined by ion chromatography using 5 ml of deionized water to extract the  
292 exposed filters. The filters were placed in glass vials containing 5 ml deionized water and were  
293 extracted for 1 hour with shaking every 5 or 6 minutes. The samples were then ready for  
294 ammonium analysis by ion chromatography.

### 295 3. Results and discussion

#### 296 3.1 Annual $\text{NH}_3$ emissions

297 Fig. 2 illustrates the trends of total  $\text{NH}_3$  emissions from 2006 to 2014 in the Yangtze River Delta.  
298 The total ammonia emissions showed an unobvious variation from 2006 to 2014 with the range  
299 from 982.95 kt to 1014.30 kt. From 2006 to 2014, nitrogen fertilizer application was the most  
300 important source of  $\text{NH}_3$  emission in the YRD, and the average emission from this source  
301 accounted for approximately 55% of the total  $\text{NH}_3$  emissions. This ratio was much higher than that  
302 reported in Fujian (39.4% in 2015, Wu et al., 2017) and the Beijing-Tianjin-Hebei region (28.6%  
303 in 2010, Zhou et al., 2015). Similar ratios have been observed in the YRD (49.3% in 2004, Dong  
304 et al., 2009) and all of China (54.0% in 2006, Dong et al., 2010). Livestock was also an important  
305 source and contributed 26-33% of the total  $\text{NH}_3$  emissions. This result was mainly attributed to the  
306 breeding of a large number of livestock. On average, nitrogen fertilizer application and livestock  
307 combined accounted for 85%-90% of the total  $\text{NH}_3$  emissions. However, the non-agricultural  
308 sources accounted for 10%-15%, which is consistent with the results of Kang et al. (2016) and Xu



309 et al. (2016).

## 310 3.2 Contributions by different sources

### 311 3.2.1 Agricultural sources

312 Figure 3 shows the estimations of  $\text{NH}_3$  emissions from nitrogen fertilizer application for the  
313 period 2006-2014. Annual  $\text{NH}_3$  emissions from nitrogen fertilizer application commonly showed a  
314 decreasing trend, with a range of 532 kt to 600 kt during 2006-2014. From Figure 3, urea  
315 application was the largest source of nitrogen fertilizer application, accounting for approximately  
316 60% of the emissions.  $\text{NH}_3$  emissions from ammonium acid carbonate (ABC) ranged from 159 kt  
317 to 202 kt and contributed to approximately 30% of the emissions from nitrogen fertilizer  
318 application.  $\text{NH}_3$  emissions from urea and ABC decreased by approximately 45 kt and 23 kt,  
319 respectively, from 2006 to 2014. It is worth noting that the emissions of  $\text{NH}_3$  from other  
320 nitrogenous fertilizers increased by approximately 17 kt from 2006 to 2014. In general, the annual  
321 variation in  $\text{NH}_3$  emissions reflects the changes in agricultural activities in the YRD. A distinct  
322 seasonal variation in  $\text{NH}_3$  emissions from nitrogen fertilizer application in the YRD in 2014 is  
323 shown in Figure 4. Obviously, the maximum  $\text{NH}_3$  emissions occurred in summer, and minimum  
324 emissions occurred in winter. The monthly  $\text{NH}_3$  emissions were highest in July, with a value of  
325 310 kt. This seasonal variation in  $\text{NH}_3$  emissions was mainly related to temperature and  
326 agricultural activities. The winter wheat-summer rice rotation or two season rice system is  
327 common farming characteristic in the YRD.  $\text{NH}_3$  volatilizations begin to rise with increasing  
328 temperatures, the new spring seeding and basal dressing fertilizer application in spring. The higher  
329 emissions occurred in summer were mostly attributed to the common contribution of higher  
330 temperature, tillering stage dressing of early rice and basal dressing of late rice. In fall, the

331 majority of crops began to be harvested, and then the winter wheat was seeded with basal dressing.  
332 Despite a large amount of fertilizer used in fall, the lower  $\text{NH}_3$  emissions were mainly related to  
333 the low temperature.

334 Ammonia emissions from livestock waste accounted for approximately 27% of the total  
335 emissions between 2006 and 2014. The livestock included beef, cattle, sheep, rabbit, buffalo,  
336 cattle, cow and poultry. As shown in Figure 5, pigs were the largest single source of livestock  $\text{NH}_3$   
337 emissions (approximately 80% of the emissions), and these emissions were significantly higher  
338 than those from other livestock sources. The second largest source was chickens, accounting for  
339 approximately 5% of livestock  $\text{NH}_3$  emissions. These results are related to people's large demand  
340 for pigs and chickens. The other livestock sources contributed approximately 15% of the  $\text{NH}_3$   
341 emissions and varied from 38.47 kt to 57.54 kt. There were relatively higher  $\text{NH}_3$  emissions from  
342 cattle and buffalo, which were due to the large amount of discharge of faecal material and urine  
343 during the breeding process. On average, the annual emissions from livestock from 2006 to 2014  
344 ranged between 255.99 kt and 328.11 kt, with the highest emissions in 2012.

#### 345 3.2.2 Non-agricultural sources

346  $\text{NH}_3$  emissions from the non-agricultural sources in the YRD between 2006 and 2014 are listed  
347 in Table 1.  $\text{NH}_3$  emissions from non-agricultural sources contributed little to the ammonia  
348 emissions over the YRD region, accounting for approximately 10%-15% of the total emission and  
349 varying from 124.64 kt to 137.23 kt. This ratio was similar to a study in Fujian (17.5% in 2015,  
350 Wu et al., 2017) and China (19% in 2012, Kang et al., 2016). Humans were the largest  
351 non-agricultural sources for  $\text{NH}_3$  emissions and contributed 37.2%-43.0% from 2006 to 2014.  
352  $\text{NH}_3$  emissions showed a declining trend for humans from 2006 to 2014, which was due to the

353 decrease in rural depopulation under sanitary conditions and demography transition. Biomass  
354 burning was the second largest non-agricultural source of  $\text{NH}_3$ , contributing from 31.02% to  
355 34.88% of the  $\text{NH}_3$  emissions from non-agricultural sources.  $\text{NH}_3$  emissions commonly showed a  
356 declining trend for humans, the chemical industry and biomass burning from 2006 to 2014, while  
357  $\text{NH}_3$  emissions increased from vehicles, garbage treatment, grassland, sewage treatment, pets and  
358 fossil burning. It is worth noting that vehicles, garbage treatment and urban grassland were the  
359 fastest growing sources of  $\text{NH}_3$  emissions, with emissions in 2014 being 2.9, 2.7 and 2.2 times  
360 higher, respectively, than those in 2006. These were mainly due to the increase in the number of  
361 vehicles, the production of more garbage with the improvement of living standards and  
362 beautifying the environment in urban construction planning. The  $\text{NH}_3$  emissions from fossil  
363 burning, sewage treatment and pets showed a slight upward trend with the city expansion. In  
364 general, the  $\text{NH}_3$  emissions from non-agricultural sources increased gradually, with the emissions  
365 in 2014 being 1.1 times those in 2006.

### 366 3.3 Contributions by city

367 The  $\text{NH}_3$  emissions from various sources and the relative contributions from 25 cities over the  
368 YRD are summarized in Figure 6. Agricultural sources were the major sources of cities in the  
369 YRD, with a total contribution of 70%~90%. Nitrogen fertilizer application was the largest source  
370 in most cities in the YRD. However, livestock contributed the most in Shanghai (40.73%),  
371 Wenzhou (43.51%) and Zhoushan (41.63%) in 2014. The average  $\text{NH}_3$  emissions of cities in the  
372 YRD reached 39.46 kt, which was much higher than that in PRD (21.74 kt in 2006, Zheng et al.,  
373 2012) and in Fujian (25.36 kt in 2015, Wu et al., 2017), but lower than that in the BTH region  
374 (121.05 kt in 2010, Zhou et al., 2015).  $\text{NH}_3$  emissions from Shanghai, Jiangsu and Zhejiang

375 provinces accounted for approximately 67.41%, 28.94% and 3.66%, respectively, of the YRD in  
376 2014. Because the extensive breeding and large planting areas, high  $\text{NH}_3$  emissions occurred in  
377 Jiangsu Province. Xuzhou had the highest  $\text{NH}_3$  emissions, followed by Yancheng and Nantong,  
378 which exceeded the average  $\text{NH}_3$  emissions by 59.84 kt, 49.30 kt and 30.35 kt, respectively. This  
379 was mainly due to the high production of livestock and poultry and the large area of cultivated  
380 agricultural land. Zhoushan had the minimum  $\text{NH}_3$  emissions and accounted for only 0.36% of the  
381 total emissions. This can be attributed to the more islands and lesser planting areas in Zhoushan.

### 382 3.4 Spatial distribution

383 The  $1 \text{ km} \times 1 \text{ km}$  gridded  $\text{NH}_3$  emissions in 2014 in the YRD region are shown in Figure 7. As  
384 shown in Figure 7a, the nitrogen fertilizer application source showed a large emission area and  
385 mainly concentrated in Jiangsu Province. It is worth noting that high  $\text{NH}_3$  emissions were found in  
386 northern areas in Jiangsu Province, which was mainly related to the large planting areas. The  $\text{NH}_3$   
387 emission was estimated to be  $4 \text{ t/km}^2$  in northern areas of Jiangsu Province, while the emission  
388 was only  $2 \text{ t/km}^2$  in most areas of Zhejiang Province and Shanghai. The  $\text{NH}_3$  emissions from  
389 livestock showed a similar trend as that observed for nitrogen fertilizer application (Figure 7b).  
390 The gridded value was below  $40 \text{ t/km}^2$  in most areas, while the gridded ammonia emission in  
391 Nantong exceeded  $80 \text{ t/km}^2$  due to the large amount of livestock. It is worth noting that there were  
392 sporadic high gridded emissions in Lishui with values over  $80 \text{ t/km}^2$ , which can be explained by  
393 the concentrated distribution of rural residential areas in Lishui.

394 The spatial distribution of ammonia emissions from humans, pets, garbage treatment, sewage  
395 treatment and domestic fuel sources was determined based on the population density to avoid  
396 unmanned areas such as oceans and forests. The gridded data of the population distribution in

397 China were obtained from the National Earth System Science Data Sharing Infrastructure. The  
398 ammonia emissions from population-related sources were concentrated in Shanghai and Jiangsu  
399 Province, while the emissions were relatively scattered in Zhejiang Province (Figure 7c). The high  
400 emission areas were mainly concentrated in Shanghai, Suzhou, Hangzhou and coastal areas of  
401 Wenzhou. Figure 7d shows that the high  $\text{NH}_3$  emissions of urban grasslands were mainly  
402 concentrated in Shanghai, Hangzhou, Suzhou and Nanjing, and were dispersed in northern areas  
403 of Jiangsu Province and southern areas of Zhejiang Province, which were related to the areas of  
404 the urban scale and grassland areas. Obviously, higher  $\text{NH}_3$  emissions from industry were  
405 concentrated in the central part of the YRD, such as Shanghai, Nanjing, Wuxi, and Suzhou (Figure  
406 7e). These cities have many industrial enterprises and relatively high energy consumption, which  
407 led to a higher level of ammonia emissions. As shown in Figure 7f, high  $\text{NH}_3$  emissions from  
408 vehicles mainly occurred in urban areas with dense populations, heavy traffic flows and crowded  
409 road networks, especially in Shanghai, Hangzhou, Wuxi and Suzhou.

410 The distribution of the agricultural sources showed a trend of high emissions in the northern  
411 area and low emissions in the southern area of the YRD, which was related to the amount of  
412 livestock and planting areas. In contrast, the high value of  $\text{NH}_3$  emissions from non-agricultural  
413 sources in the YRD was concentrated in Shanghai with a gridded value higher than  $8 \text{ t/km}^2$ , while  
414 the gridded value was less than  $2 \text{ t/km}^2$  in most areas of the YRD. Obviously, this result was  
415 related to the emissions from humans and vehicles, which accounted for 37.27% and 21.99%,  
416 respectively, of  $\text{NH}_3$  emissions from the non-agricultural sources in Shanghai.

417 3.5 Comparison with previous estimates

418 The comparison of ammonia emissions in different regions is listed in Table 2. Consistent with  
419 the results of most studies, nitrogen fertilizer application was the largest source of  $\text{NH}_3$  emissions  
420 in the YRD. The total emission in this study was calculated to be 1002.52 kt in 2006, which is less  
421 than that calculated by Dong et al. (2010) and higher than that calculated by Huang et al. (2012) in  
422 the same base year. This was mainly due to the differences in the emission sources and emission  
423 factors. Dong et al. (2010) used uniform emission factors for the same source over China, and  
424 these factors were derived mainly from European experiments rather than domestic measurements  
425 in China. The 5 ammonia emission sources (nitrogen fertilizer application, livestock, humans,  
426 vehicles and the industrial process of nitrogen fertilizer production) were considered in the studies  
427 by Wang et al. (1997), Dong et al. (2009) and Dong et al. (2010). In this study, we considered  
428 more  $\text{NH}_3$  sources (domestic fuel, grassland and pets). In addition, some localized revision for  
429 nitrogen fertilizer application sources was made in the calculation of emission factors based on the  
430 local soil pH, temperature and some agricultural practices. The revised emission factors can better  
431 reflect the actual  $\text{NH}_3$  emission of the nitrogen fertilizer application in the YRD.

### 432 3.6 Uncertainty analysis of $\text{NH}_3$ emissions

433 The uncertainties of the emission inventory were due to the lack of some activity levels and  
434 localized emission factors. The uncertainties of  $\text{NH}_3$  emissions from various sources are listed in  
435 Table 3. Relatively high uncertainties were associated with livestock (-58%, 114%) and garbage  
436 treatment (-52%, 72%) sources. The higher uncertainty among these sources is mainly due to the  
437 following: (1) the emission factors were mainly from other research results and showed  
438 differences in different studies, especially for livestock. The emission factors were selected as the  
439 converted mean value, but there were differences in emission factors through different breeding

440 methods. (2) In this study, the data related to cattle, buffalo and poultry data in some cities were  
441 calculated using provincial data because of the incomplete statistics in the statistical yearbook.  
442 The inaccuracy of source-level classification was also another reason for the uncertainty. More  
443 detailed parameters cannot be obtained from the statistical yearbook, such as the proportion of  
444 chickens and ducks. (3) In addition, there was great uncertainty in garbage treatment due to the  
445 emissions from the amount of  $\text{CH}_4$  released from the landfill process. Compared with other studies,  
446 the reliability of ammonia emissions from nitrogen sources is higher because of the use of  
447 localized emission factors. As numerous parameters, including temperature, pH, precipitation,  
448 application rate and landuse, were considered in nitrogen fertilizer application, the uncertainty was  
449 relatively small. The overall estimated range of  $\text{NH}_3$  emission was 496.29 kt to 1784.33 kt,  
450 corresponding to uncertainties of -55% to 60%.

### 451 3.7 Characteristics of ambient $\text{NH}_3$ concentration

452 The  $\text{NH}_3$  emissions in Nanjing in 2014 were compared with the observed data. As shown in  
453 Figure S1, the concentration of observed  $\text{NH}_3$  showed obvious seasonal variation, and the ranking  
454 of the seasonal average concentration was summer ( $19.25 \mu\text{g}\cdot\text{m}^{-3}$ ) > autumn ( $15.33 \mu\text{g}\cdot\text{m}^{-3}$ ) >  
455 spring ( $12.54 \mu\text{g}\cdot\text{m}^{-3}$ ) > winter ( $9.89 \mu\text{g}\cdot\text{m}^{-3}$ ). The observed  $\text{NH}_3$  concentration in summer was  
456 twice as high as that in winter. The  $\text{NH}_3$  concentration distribution peaked in the warm season and  
457 decreased to the lowest value in the coldest season. To compare and analyse the time variation in  
458 ammonia emissions, we analysed the molar ratios of  $(2\text{SO}_2 + \text{NO}_2)/\text{NH}_3$  from September 2015 to  
459 August 2016 in Nanjing. The molar ratio was used to determine the state of  $\text{NH}_3$ ; for example,  $\text{NH}_3$   
460 is suggested to be deficient when the value is greater than 1. The molar ratios from June to August  
461 were lower than that from other months, indicating that ammonia emissions in summer are higher

462 than in other months. This change was consistent with the trend of the emission inventory in this  
463 study.

464 In addition, linear regression analysis was performed to investigate the relationship of the  
465 observed  $\text{NH}_3$  concentrations with  $\text{NH}_3$  emission density and temperature (Figure S2). The results  
466 showed that the observed  $\text{NH}_3$  concentration increased with temperature ( $R^2 = 0.79$ ) and  
467 transformed  $\text{NH}_3$  emission density ( $R^2 = 0.57$ ). The relationship suggests that the observed  $\text{NH}_3$   
468 concentrations displayed a moderate correlation with temperature and  $\text{NH}_3$  emission density. This  
469 may be explained by the fact that the observed  $\text{NH}_3$  concentration can be affected by the  
470 temperature, rainfall and position of the passive sampler. Further multi-site observations are  
471 required to quantify the contributions of local sources to the ambient  $\text{NH}_3$  concentrations and  
472 spatial-temporal variations.

#### 473 4. Conclusions

474 A comprehensive  $\text{NH}_3$  emission inventory from 2006 to 2014 was developed based on activity  
475 data and specific EFs for agricultural and non-agricultural sources. Generally, the total ammonia  
476 emissions changed insignificantly between 2006 and 2014. The annual variations in emissions  
477 were mainly attributed to the type of fertilizer and the management of livestock. The  $\text{NH}_3$  from  
478 nitrogen fertilizer application showed a decreasing trend, while the  $\text{NH}_3$  from livestock showed an  
479 increasing trend.  $\text{NH}_3$  emissions generally peaked in summer, corresponding to the planting  
480 schedule and relatively high temperature. Vehicles were calculated to be the fastest growing  
481 non-agricultural source in  $\text{NH}_3$  emission inventory. In addition, the spatial grid allocation of the  
482 ammonia emission inventory was also carried out from point, area and line sources. The spatial  
483 pattern of the total emissions has been basically the same in recent years, with a trend of higher



484 emissions in the northern area and lower emissions in the southern area of the YRD region.

485 The uncertainty range of emissions in the YRD was -55% to 60% using Monte Carlo simulation  
486 with 95% confidence. The assessments of uncertainty demonstrated that high uncertainty occurred  
487 in the emissions of livestock and waste treatment. Moreover, the seasonal averaged  $\text{NH}_3$   
488 concentration in Nanjing ranked in the order of summer > autumn > spring > winter. The molar  
489 ratio of  $(2\text{SO}_2 + \text{NO}_2)/\text{NH}_3$  was consistent with the emission density of our study. A moderate  
490 correlation was observed between  $\text{NH}_3$  concentration and temperature and  $\text{NH}_3$  emission density.

491 Our results were different from previous published studies in this region, probably due to the  
492 selection of EFs and emission sources. There were still gaps in the results of emission inventories  
493 due to the lack of some activity data and emission factors. Therefore, our inventories should be  
494 further improved, especially for the estimation of ammonia emissions from agricultural sources.

#### 495 **Acknowledgments**

496 This work was supported by the National Key Research and Development Program of China  
497 (No. 2019YFC0214604 and 2016YFC0203501), the National Natural Science Foundation of  
498 China (No. 41775154), and Six Talent Peaks Project in Jiangsu Province (No. JNHB-057).

#### 499 **References**

- 500 Anderson, N., Strader, R., Davidson, C., 2003. Airborne reduced nitrogen: ammonia emissions from agricultural  
501 and other sources. *Environ. Int.*, 19, 3873-3883.
- 502 Andrea, R., Corry de Keizer., Jeroen P. Van der Sluijs., et al., 2008. Monte carlo analysis of uncertainties in the  
503 netherlands greenhouse gas emission inventory for 1990-2004. *Atmos. Environ.*, 42, 8263-8272.
- 504 Bouwman, A.F., Lee, D.S., Asman, W.A.H., et al., 1997. A global high-resolution emission inventory for ammonia.  
505 *Global Biogeochem. Cy.*, 11, 561-587.

- 506 Battye, W., Aneja, V.P., Roelle, P.A., 2003. Evaluation and improvement of ammonia emissions inventories. *Atmos.*  
507 *Environ.*, 37, 3873-3883.
- 508 Che, W.W., 2010. A highly resolved mobile source emission inventory in the Pearl River Delta and assessment of  
509 motor vehicle. South China University of Technology, Guangzhou, China. (in Chinese)
- 510 Chen, Y., 2017. Ionic characteristic of atmospheric particles and precipitation in Shanghai. Shanghai Normal  
511 University, Shanghai, China. (in Chinese)
- 512 DEFRA (Department for Environment, Food and Rural Affairs), 2001. National Ammonia Reduction and Strategy  
513 Evaluation System (NARSES). Project AM0101.
- 514 Dong, Y.Q., Chen, C.H., Huang, C., et al., 2009. Anthropogenic emission and distribution of ammonia over the  
515 Yangtze River Delta. *Acta Sci. Circumstantiae*, 29(8), 1611-1671. (in Chinese)
- 516 Dong, W.X., Xing, J., Wang, S.X., 2010. Temporal and Spatial Distribution of Anthropogenic Ammonia Emissions  
517 in China: 1994-2006. *Environ. Sci.*, 31, 1457-1463. (in Chinese)
- 518 EEA (European Environment Agency), 2013. EMEP/EEA Air Pollutant Emission Inventory Guidebook 2013, Tech.  
519 Rep. 12/2013, Copenhagen.
- 520 Feng, X.Q., Wang, X.R., He, M., et al., 2015. A 2012-based anthropogenic ammonia emission inventory and its  
521 spatial distribution in Sichuan Province. *Acta Sci. Circumstantiae*, 35, 394-401 (in Chinese).
- 522 Gu, Y.Y., Wang, B.G., Yang, J., et al., 2012. Ammonia source and emission factor in municipal wastewater  
523 treatment plant. *Environ. Chem.*, 31, 146-151. (in Chinese)
- 524 Huang, X., Qiu, R., Chan, C.K., et al., 2011. Evidence of high PM<sub>2.5</sub> strong acidity in ammonia-rich atmosphere of  
525 Guangzhou, China. Transition in pathways of ambient ammonia to from aerosol ammonia at  $[\text{NH}_4^+]/[\text{SO}_4^{2-}]=1.5$ .  
526 *Atmos. Res.*, 99,488-495.

- 527 Huang, X., Song, Y., Li, M.M., et al., 2012. A high-resolution ammonia emission inventory in China. *Global*  
528 *Biogeochem. Cy.*, 26, GB1030,
- 529 Huang, R.J., Zhang, Y., Bozzetti, C., et al., 2014. High secondary aerosol contribution to particulate pollution  
530 during haze events in China. *Nature*, 514, 218-222.
- 531 Krupa, S.V., 2003. Effects of atmospheric ammonia (NH<sub>3</sub>) on terrestrial vegetation: a review. *Environ. Pollut.*, 124,  
532 179-221.
- 533 Kang, Y.N., Liu, M.X., Song, Y., et al., 2016. High-resolution ammonia emissions inventories in China from 1980  
534 to 2012. *Atmos. Chem. Phys.*, 16, 2043-2058.
- 535 Matson, P., Lohse, K.A., Hall, S.J., 2002. The globalization of nitrogen deposition: consequences for terrestrial  
536 ecosystems. *Ambio*, 31, 113-119.
- 537 Meng, Z.Y., Lin, W.L., Jiang, X.M., et al., 2011. Characteristics of atmospheric ammonia over Beijing, China.  
538 *Atmos. Chem. Phys.*, 11, 6139-6151.
- 539 Ministry of Ecology and Environment of the People's Republic of China. Technical Guidelines for Preparation of  
540 Atmospheric Ammonia Emission Inventory (for Trial Implementation). 2014-8-19.  
541 <http://www.mee.gov.cn/gkml/hbb/bgg/201408/W020140828351293771578.pdf>
- 542 Olivier, J.G.J., Bouwman, A.F., Van Der Hoek, K.W., et al., 1998. Global air emission inventories for  
543 anthropogenic sources of NO<sub>x</sub>, NH<sub>3</sub> and N<sub>2</sub>O in 1990. *Environ. Pollut.*, 102, 135-148.
- 544 Pan, Y.P., Wang, Y.S., Tang, G.Q., et al., 2012. Wet and dry deposition of atmospheric nitrogen at ten sites in  
545 Northern China. *Atmos. Chem. Phys.*, 12, 6515-6535.
- 546 Shen, X.L., 2014. A highly resolved anthropogenic ammonia emission inventory in Guangdong Province and  
547 assessment of control strategies. South China University of Technology, Guangzhou, China (in Chinese).

- 548 Streets, D.G., Bond, T.C., Garmichael, G.R., et al., 2003. An inventory of gaseous and primary aerosol emissions in  
549 Asia in the year 2000. *J. Geophys. Res.*, 108(21), 8809.
- 550 Sarwar, G., Corsi R.L., Kinney, K. A., et al., 2005. Measurements of ammonia emissions from oak and pine forests  
551 and development of a non-industrial ammonia emissions inventory in Texas. *Atmos. Environ.*, 39, 7137-7153.
- 552 Sutton, M.A., Dragosits, U., Tang, Y.S., et al., 2000. Ammonia emissions from non-agricultural sources in the UK.  
553 *Atmos. Environ.*, 34,856-863.
- 554 Tian, M.A., Wang, H.B., Chen, Y., et al., 2016. Characteristics of aerosol pollution during heavy haze events in  
555 Suzhou, China. *Atmos. Chem. Phys.*, 16, 7357-7371.
- 556 Van Der Hoke, K.W., 1998. Estimating ammonia emission factors in Europe: summary of the Work of the UNECE  
557 Ammonia Expert Panel. *Atmos. Environ.*, 32, 315-316.
- 558 Wang, X.W., Lu, X.F., Pang, Y.B., et al., 1997. Geographical Distribution of NH<sub>3</sub> emission inventories in China,  
559 *Acta Scientiae Circumstantiae*, 17, 2-7. (in Chinese)
- 560 Wang, S.X., Xing, J., Jang, C., et al., 2011. Impact assessment of ammonia emissions on inorganic aerosols on  
561 inorganic aerosols in East China using response surface modeling technique. *Environ. Sci. Tec.*, 45, 9293-9300.
- 562 Chinkin, L.R. and Ryan, P.A., 2002. Recommended Improvements to the CMU Ammonia Emission Inventory  
563 Model for Use by LADCO. (Prepared for Lake Michigan Air Directors Consortium).
- 564 Wu, S.P., Zhang, Y.J., Schwab, J.J., et al., 2017. High-resolution ammonia emissions inventories in Fujian, China,  
565 2009-2015. *Atmos. Environ.*, 162, 100-14.
- 566 Wang, K., Cao, J.J., Tian H.Z., et al., 2017. An emission inventory spatial allocate method based on POI data.  
567 *China Environ. Sci.*, 37(6), 2377-2382. (in Chinese)
- 568 Wang, R.J., Wang, K., Zhang, F., et al., 2017. Emission Characteristics of Vehicles from National Roads and  
569 Province in China. *Environ. Sci.*, 38(9), 3553-3560. (in Chinese)

- 570 Wang, R.Y., Ye, X.N., Liu, Y.X., et al., 2018. Characteristics of atmospheric ammonia and its relationship with  
571 vehicle emissions in a megacity in China. *Atmos. Environ.*, 182, 97-104.
- 572 Wang, C., Yin, S.S., Bai, L., et al., 2018. High-resolution ammonia emission inventories with comprehensive  
573 analysis and evaluation in Henan, China, 2006-2016, *Atmos. Environ.*, 193, 11-23.
- 574 Wang, C., 2015. Characteristics and prediction research of automobile emissions in Shandong province based on  
575 COPERT4 model. Ocean University of China, Qingdao, China. (in Chinese)
- 576 Xu, P., Liao, Y.J., Lin, Y.H., et al., 2016. High-resolution inventory of ammonia emissions from agricultural  
577 fertilizer in China from 1978 to 2008. *Atmos. Chem. Phys.*, 16, 1207-1218.
- 578 Yu, X.N., Shen, L., Xiao, S.H., et al., 2019. Chemical and Optical Properties of Atmospheric Aerosols during the  
579 Polluted Periods in a Megacity in the Yangtze River Delta, China. *Aerosol Air Qual. Res.*, 19, 103-117.
- 580 Zhang, M.S. and Luan, S.J., 2009. Application of NARSES in evaluation of ammonia emission from nitrogen  
581 fertilizer application in planting system in China. *J. Anhui Agr. Sci.*, 37, 3583-3586. (in Chinese)
- 582 Zhang, Y.S., Luan, S.J., Chen, L.L., et al., 2011. Estimating the volatilization of ammonia from synthetic  
583 nitrogenous fertilizers used in China. *J. Environ. Manage.*, 92, 480-493.
- 584 Zhang, L., Chen, Y., Zhao, Y., et al., 2018. Agricultural ammonia emissions in China: reconciling bottom-up and  
585 top-down estimates. *Atmos. Chem. Phys.*, 18, 339-355.
- 586 Zhang, Y., Dore, A.J., Ma, L., et al., 2010. Agricultural ammonia emissions inventory and spatial distribution in the  
587 North China Plain. *Environ. Pollut.*, 158, 490-501.
- 588 Zhang, S., Wu, Y., Liu, H., et al., 2013. Historical evaluation of vehicle emission control in Guangzhou based on a  
589 multi-year emission inventory. *Atmos. Environ.*, 76, 32-42.
- 590 Zhao, X.F., 2019. Positioning observation and regional simulation of atmospheric nitrogen emission and deposition.  
591 Nanjing University, Nanjing, China. (in Chinese)

- 592 Zheng, J.Y., Yin, S.S., Kang, D.W., et al., 2012. Development and uncertainty analysis of a high-resolution NH<sub>3</sub>  
593 emissions inventory and its implications with precipitation over the Pearl River Delta region, China. *Atmos. Chem.*  
594 *Phys.*, 12, 7041-7058.
- 595 Zhou, Y., Cheng, S.Y., Lang J.L., et al., 2015. A comprehensive ammonia emission inventory with high-resolution  
596 and its evaluation in the Beijing-Tianjin-Hebei (BTH) region, China. *Atmos. Environ.*, 106, 305-317.

Journal Pre-proof

1 High-resolution anthropogenic ammonia emission inventory for the Yangtze River

2 Delta, China

3 Xingna Yu<sup>1,\*</sup>, Li Shen<sup>1,2</sup>, Xinhong Hou<sup>1</sup>, Liang Yuan<sup>3</sup>, Yuepeng Pan<sup>4</sup>, Junlin An<sup>1</sup>, Shuqi Yan<sup>1</sup>

4

5 **Tables:**

6 Table 1. Contributions to NH<sub>3</sub> emissions (kt) from non-agricultural sources in the YRD from  
7 2006 to 2014

8 Table 2. Comparison of NH<sub>3</sub> emissions (kt·yr<sup>-1</sup>) with other published results in the YRD

9 Table 3. Uncertainty of ammonia emissions from various sources in the YRD in 2014

10 Table 1. Contributions to NH<sub>3</sub> emissions (kt) from non-agricultural sources in the YRD from 2006 to 2014.

11		2006	2007	2008	2009	2010	2011	2012	2013	2014
	Humans	55.02	52.16	52.14	52.10	51.42	51.35	51.24	51.18	51.11
	Chemical industry	9.94	10.42	9.74	11.72	8.92	8.81	9.86	9.59	8.99
	Fossil burning	6.74	6.74	6.30	6.39	6.52	6.80	6.97	6.94	7.37
	Biomass burning	44.71	43.76	42.80	40.33	42.56	41.95	42.74	42.73	42.57
	Garbage treatment	1.66	1.87	1.99	2.51	2.75	2.89	3.44	3.61	4.51
	Sewage treatment	1.36	1.48	1.71	1.81	1.91	2.01	2.14	2.17	2.17
	Vehicles	5.15	5.22	5.95	7.10	8.52	10.04	11.48	13.26	14.89
	Pets	2.39	2.47	2.53	2.60	2.78	2.84	2.89	2.94	2.99
	Urban grassland	1.21	1.38	1.50	2.06	2.14	2.32	2.47	2.53	2.63
	Total	128.18	125.5	124.66	126.62	127.52	129.01	133.23	134.95	137.23



12

Table 2. Comparison of NH<sub>3</sub> emissions (kt·yr<sup>-1</sup>) with other published results in the YRD

Base Year	Total	Nitrogen					others	
		Fertilizer application	Livestock	Humans	Vehicles			
1991	711.41	226.85	314.65	160.22	—	9.69	Wang et al,	
2004	460.68	227.33	203.28	4.11	—	25.96	Dong et al., 2009	
2006	1416.22	957.06	364.64	87.10	—	7.42	Dong et al., 2010	
2006	607.70	305.10	202.30	12.10	10.70	84.90	Huang et al., 2016	
2006	1002.52	584.23	290.10	55.02	5.15	68.02	This study	
2014	986.73	532.82	316.68	51.11	14.89	71.24	This study	

13

14

15

Table 3. Uncertainty of ammonia emissions from various sources in the YRD in 2014

Source	Emission (kt)	Mean (kt)	Uncertainty range
Nitrogen fertilizer application	532.82	586.71	[-47%, +68%]
Livestock	316.68	391.63	[-58%, +114%]
Industry	8.99	7.49	[-49%, +27%]
Fossil burning	7.37	7.39	[-42%, +60%]
Traffic	14.89	12.77	[-60%, +86%]
Garbage treatment	4.51	4.40	[-52%, +72%]
Sewage treatment	2.17	2.20	[-46%, +67%]
Human	51.11	56.44	[-34%, +71%]
Biomass	42.57	40.20	[-36%, +40%]
Grassland	2.63	2.25	[-39%, +42%]
Pets	2.99	2.91	[-36%, +47%]
Total	986.73	1114.39	[-55%, +60%]

16

1 High-resolution anthropogenic ammonia emission inventory for the Yangtze River

2 Delta, China

3 Xingna Yu<sup>1,\*</sup>, Li Shen<sup>1,2</sup>, Xinhong Hou<sup>1</sup>, Liang Yuan<sup>3</sup>, Yuepeng Pan<sup>4</sup>, Junlin An<sup>1</sup>, Shuqi Yan<sup>1</sup>

4

5 **Figures:**

6 Figure 1. Location and administrative divisions of the Yangtze River Delta region

7 Figure 2. Interannual variation in total NH<sub>3</sub> emissions in the YRD from 2006 to 2014

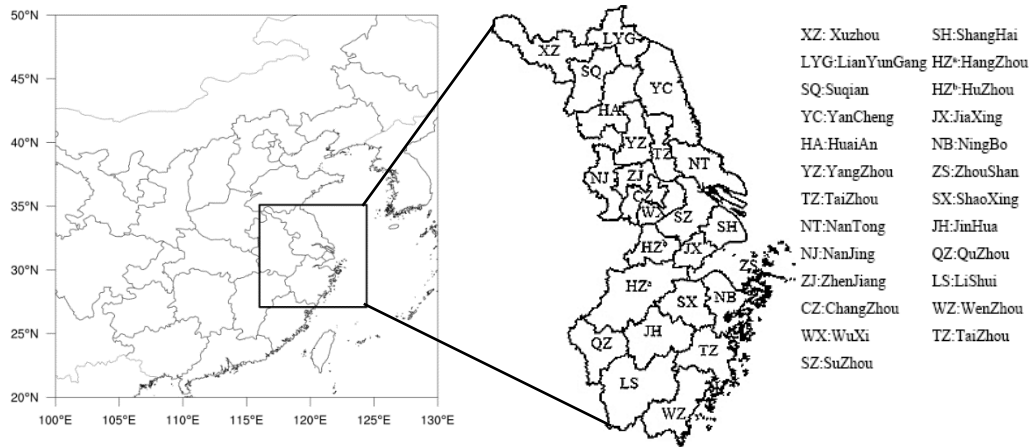
8 Figure 3. Annual variation in total NH<sub>3</sub> emissions from nitrogen fertilizer application in the YRD  
9 from 2006 to 2014

10 Figure 4. Monthly variation of ammonia emissions from nitrogen fertilizer application in the YRD in  
11 2014

12 Figure 5. Interannual variation in total NH<sub>3</sub> emissions from livestock waste in the YRD region from  
13 2006 to 2014

14 Figure 6. City-specific NH<sub>3</sub> emissions from different sources in the Yangtze River Delta in 2014

15 Figure 7. Spatial distribution of the major NH<sub>3</sub> sources and the total emission in a 1 km × 1 km grid  
16 cell in the Yangtze River Delta



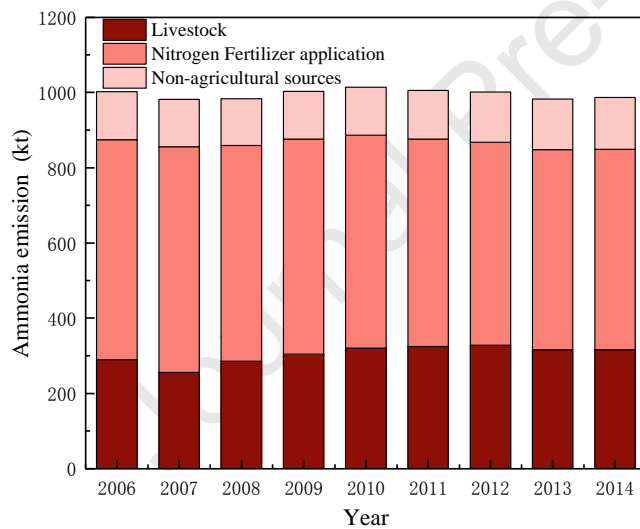
17

18 Figure 1. Location and administrative divisions of the Yangtze River Delta region

19

20

21



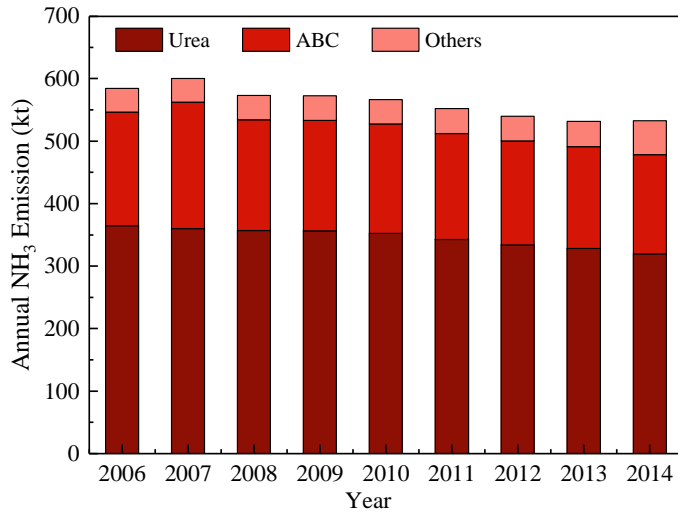
22

23 Figure 2. Interannual variation in total NH<sub>3</sub> emissions in the YRD from 2006 to 2014. The sources of emissions

24 were divided into three categories: nitrogen fertilizer application, livestock, and non-agricultural sources (humans,

25 chemical industry, fossil burning, biomass burning, garbage treatment, sewage treatment, vehicles, pets and urban

26 grassland)



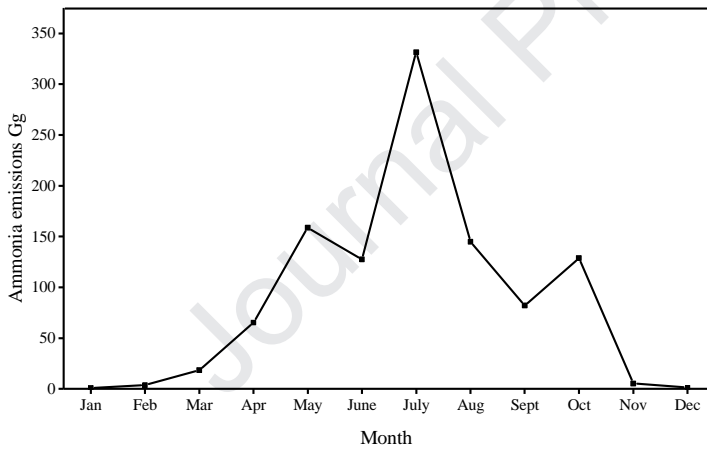
27

28 Figure 3. Annual variation in total NH<sub>3</sub> emissions from nitrogen fertilizer application in the YRD from 2006 to

29 2014. The types of sources included urea, ABC, and other nitrogenous fertilizers.

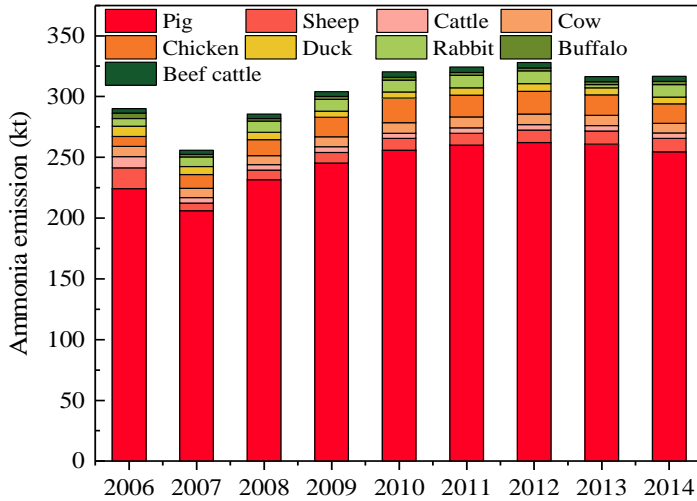
30

31



32

33 Figure 4. Monthly variation of ammonia emissions from nitrogen fertilizer application in the YRD in 2014.



34

35 Figure 5. Interannual variation in total NH<sub>3</sub> emissions from livestock waste in the YRD region from 2006 to 2014.

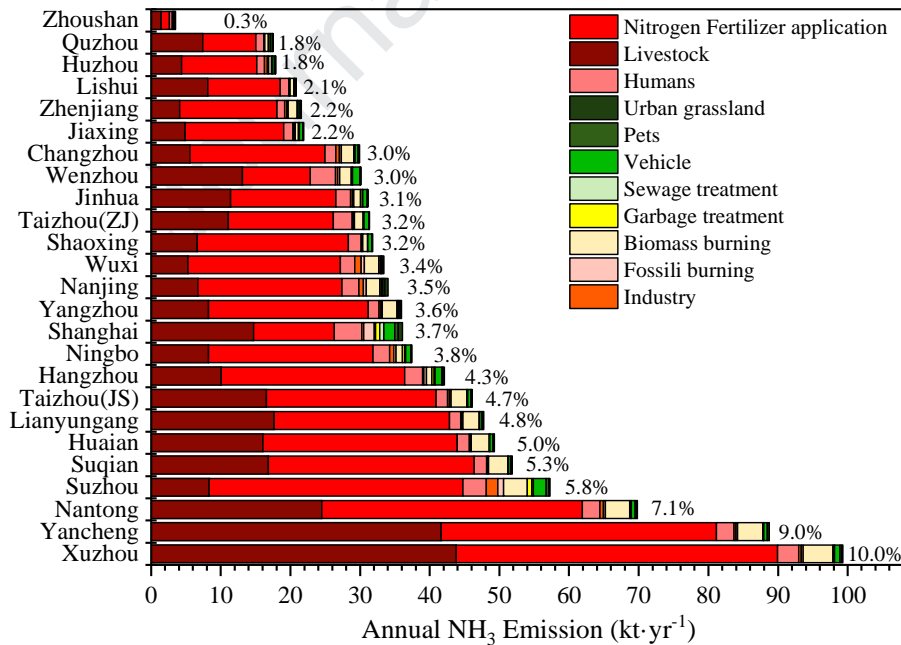
36 The types of sources included duck, chicken, rabbit, sheep, pig, buffalo, cattle, cow and beef cattle.

37

38

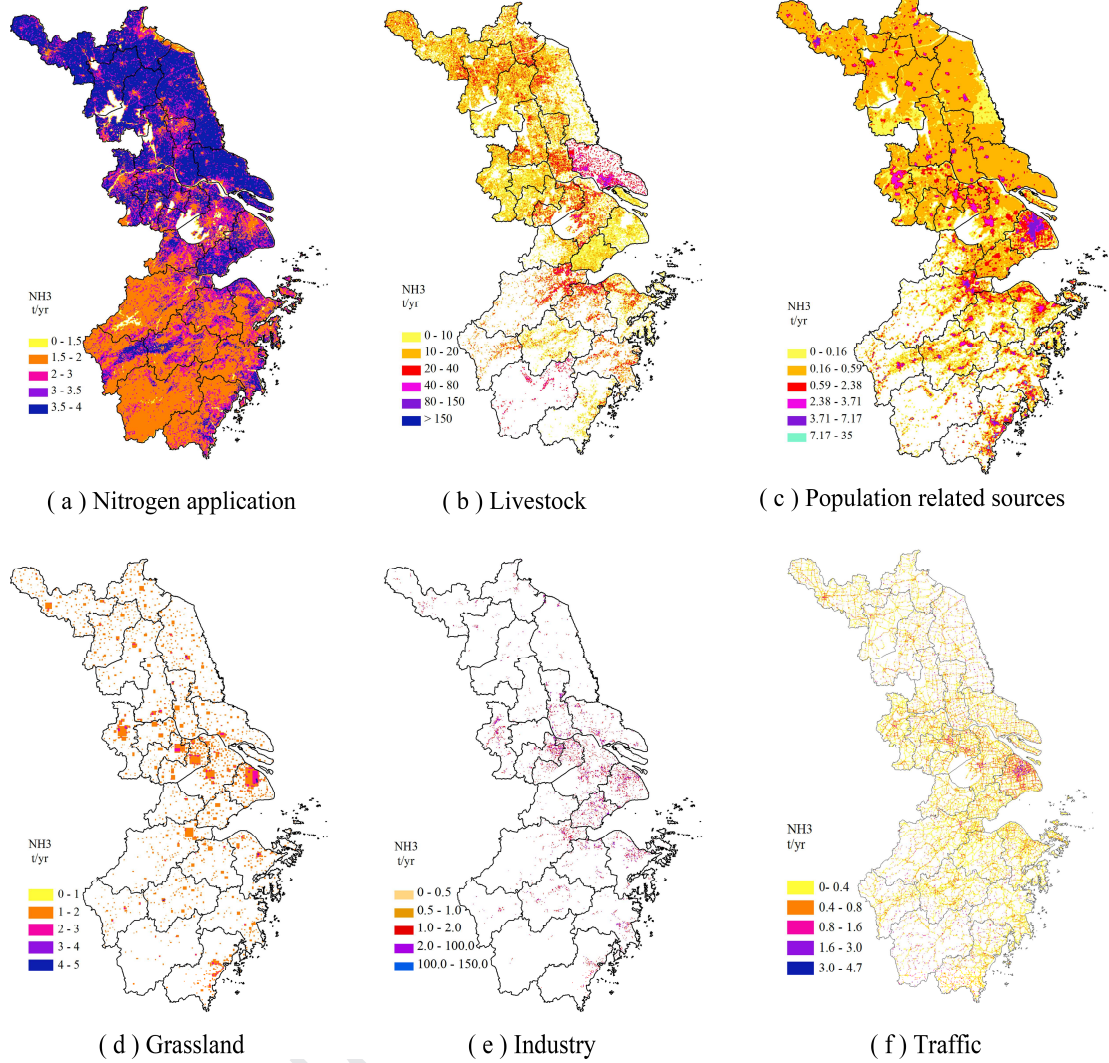
39

40



41

42 Figure 6. City-specific NH<sub>3</sub> emissions from different sources in the Yangtze River Delta in 2014.



43

44

45

46

Figure 7. Spatial distribution of the major NH<sub>3</sub> sources and the total emission in a 1 km × 1 km grid cell in the Yangtze River Delta (2014). Non-point sources include humans, pets, garbage treatment, waste treatment and civilian fossil fuels.

1

## Highlights

- 2 1. The  $1\text{km}\times 1\text{km}$  gridded  $\text{NH}_3$  emission inventory was developed based on county-level
- 3 activity data.
- 4 2. The emission of ammonia in the YRD was 998.83 kt in 2014.
- 5 3. Uncertainty and correlation analysis were used to evaluate the inventory.

Journal Pre-proof

**Declaration of interests**

The authors declare that they have no known competing financial interests or personal relationships that could have appeared to influence the work reported in this paper.

The authors declare the following financial interests/personal relationships which may be considered as potential competing interests: